Life Sciences 231 (2019) 116541

Contents lists available at ScienceDirect

Life Sciences

journal homepage: www.elsevier.com/locate/lifescie

Role of PGRMC1 in cell physiology of cervical cancer

Chuan-Chi Shih[a,1], Hsiu-Chuan Chou[b,1], Ying-Jen Chen[c], Wen-Hung Kuo[d], Chia-Hao Chan[a], Yi-Chieh Lin[c], En-Chi Liao[c], Shing-Jyh Chang[a,*], Hong-Lin Chan[c,**]

[a] Department of Obstetrics and Gynecology, Hsinchu MacKay Memorial Hospital, Hsinchu, Taiwan
[b] Department of Biomedical Engineering and Environmental Sciences, National Tsing Hua University, Taiwan
[c] Dept. of Medical Sciences & Inst. of Bioinformatics and Structural Biology, National Tsing Hua University, Hsinchu, Taiwan
[d] Department of Surgery, National Taiwan University Hospital, Taipei, Taiwan

ARTICLE INFO

Keywords:
PGRMC1
Cervical cancer
Proteomics
Metastasis

ABSTRACT

Aims: The most frequent cancers among women worldwide. The mortality of cervical cancer has declined significantly primarily due to the widespread use of Pap smear tests as a screening test and therapeutic vaccination. However, cervical cancer still remains a severe disease among the female population, as the prognosis of metastatic cervical cancer is very poor.

Key methods: In this study, we performed 2D-DIGE and MALDI-TOF/TOF MS to analyze differentially expressed proteins between HeLa and invasive HeLa-I5 cells..

Key findings: According to our proteomics data, 68 differentially expressed proteins between the HeLa and HeLa-I5 cells were identified. One of these differentially expressed proteins, Progesterone receptor membrane component 1 (PGRMC1), was selected as a candidate for further studies. To correlate the role of PGRMC1 with cellular migration and cancer progression, small interfering RNA (siRNA) was used to knockdown the expression of PGRMC1. Similar function of PGRMC1 was also observed in two other cervical cancer lines, CaSki and ME-180.

Significance: PGRMC1 plays an essential role in regulating cancer progression and metastasis of cervical cancer cells, thus serving as a potential therapeutic target for cervical cancer.

1. Introduction

On the basis of histology, cervical cancers are classified into squamous cell carcinoma, adenocarcinoma, adenosquamous carcinoma, and small cell cancer. Squamous cell carcinoma is the predominant type of cervical cancer accounting for up to 80% of all cervical cancers [1]. It starts in the squamous cells that cover the outer surface of the cervix. Because of the well-defined screening programs and treatment strategies (surgery, radiotherapy or chemotherapy), once the cervical cancer is diagnosed and treated at early stage, the 5-year survival rate of patient can be up to 80%. However, the prognosis is poor if it is diagnosed at metastatic stage. Metastasis in cervical cancer can be hematogenous or lymphatic and occurs in lymph nodes or distant organs such as lung, liver, bone, and brain. Due to the lack of any standard treatment for patients with secondary site metastasis, 5-year survival rate can be decreased up to 50% [2].

As a result, metastasis is the leading cause of cervical cancer-related mortality. Hence, it is crucial to investigate the underlying mechanism of metastasis in cervical cancer to develop effective treatment strategies.

In general, metastasis of highly invasive tumor cells from the primary tumor site to distant organs is responsible for up to 90% of cancer-associated mortality. During metastatic dissemination, first the primary tumor cells invade the surrounding tissue, and intravasate the microvasculature of the circulatory and lymphatic systems. Next, they translocate through the bloodstream followed by extravasation at distant capillary beds and colonization at secondary site leading to secondary tumor formation. The epithelial-mesenchymal transition (EMT) plays a critical role during cancer progression [3], as it allows tumor cells to acquire the capacity to invade surrounding tissue and metastasize to distant sites. During EMT, the tumor cell state changes from epithelial to mesenchymal by altering its polarity, weakening cell-to-

* Corresponding author at: Department of Obstetrics and Gynecology, Hsinchu MacKay Memorial Hospital, Hsinchu, Taiwan.
** Correspondence to: H. L. Chan, Dept. of Medical Sciences & Inst. of Bioinformatics and Structural Biology, National Tsing Hua University, Hsinchu, Taiwan, No.101, Kuang-Fu Rd. Sec.2, Hsin-chu 30013, Taiwan.
E-mail addresses: justine3@ms8.hinet.net (S.-J. Chang), hlchan@life.nthu.edu.tw (H.-L. Chan).
[1] Equal contribution of these authors.

https://doi.org/10.1016/j.lfs.2019.06.016
Received 22 April 2019; Received in revised form 31 May 2019; Accepted 5 June 2019
Available online 16 June 2019
0024-3205/

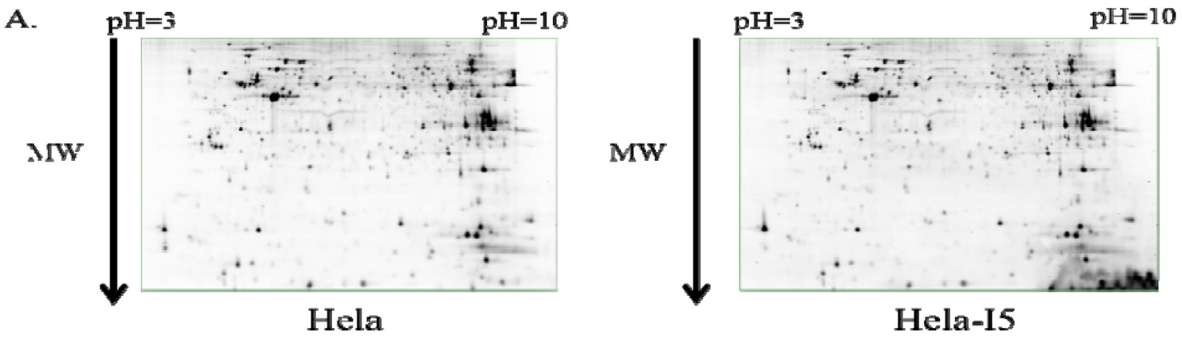

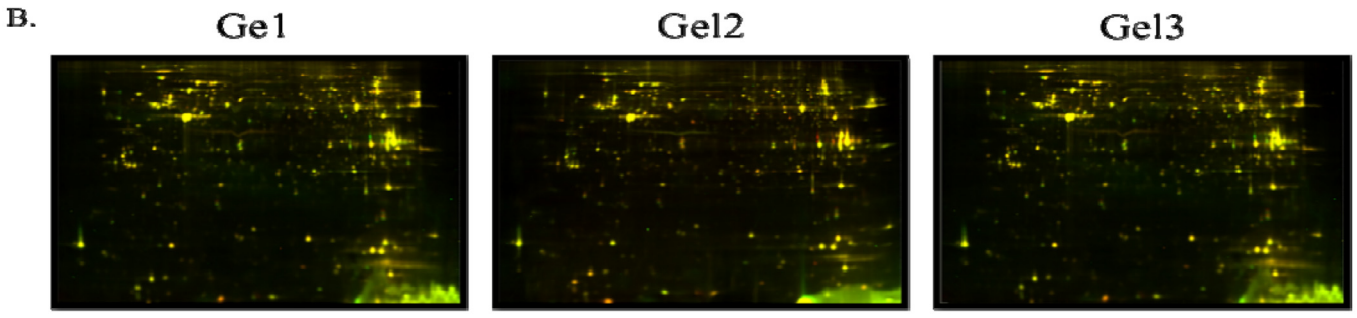

C.

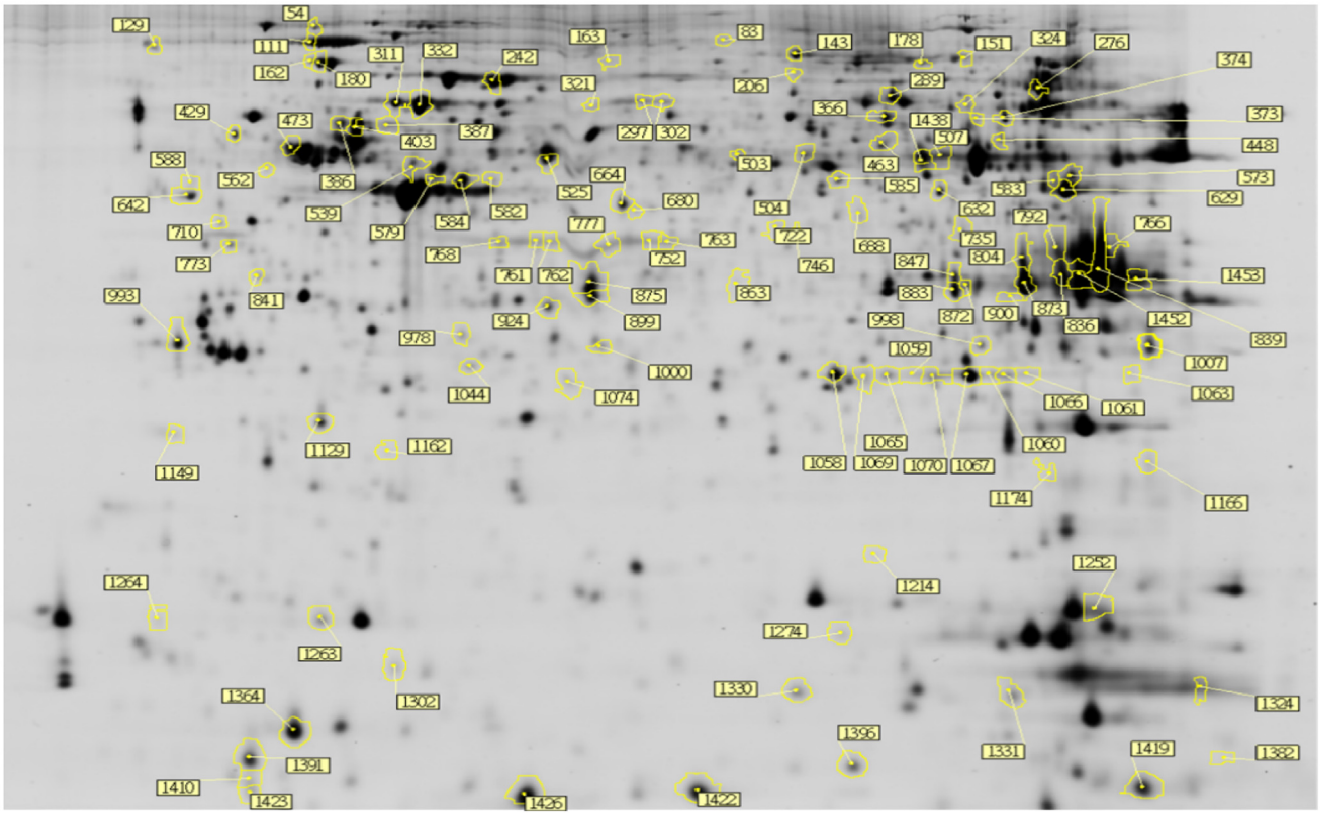

Fig. 1. Proteomic analysis between Hela and Hela-I5 cells. (A)2D-DIGE images of Hela and Hela-I5 cells were profiled by Ettan DIGE Imager. (B) Three replicate gel images of HeLa and HeLa-I5 proteins labeled with lysine-labeled Cy dyes. (C) The differentially expressed and identified proteins between HeLa and HeLa-I5 were annotated with spot numbers.

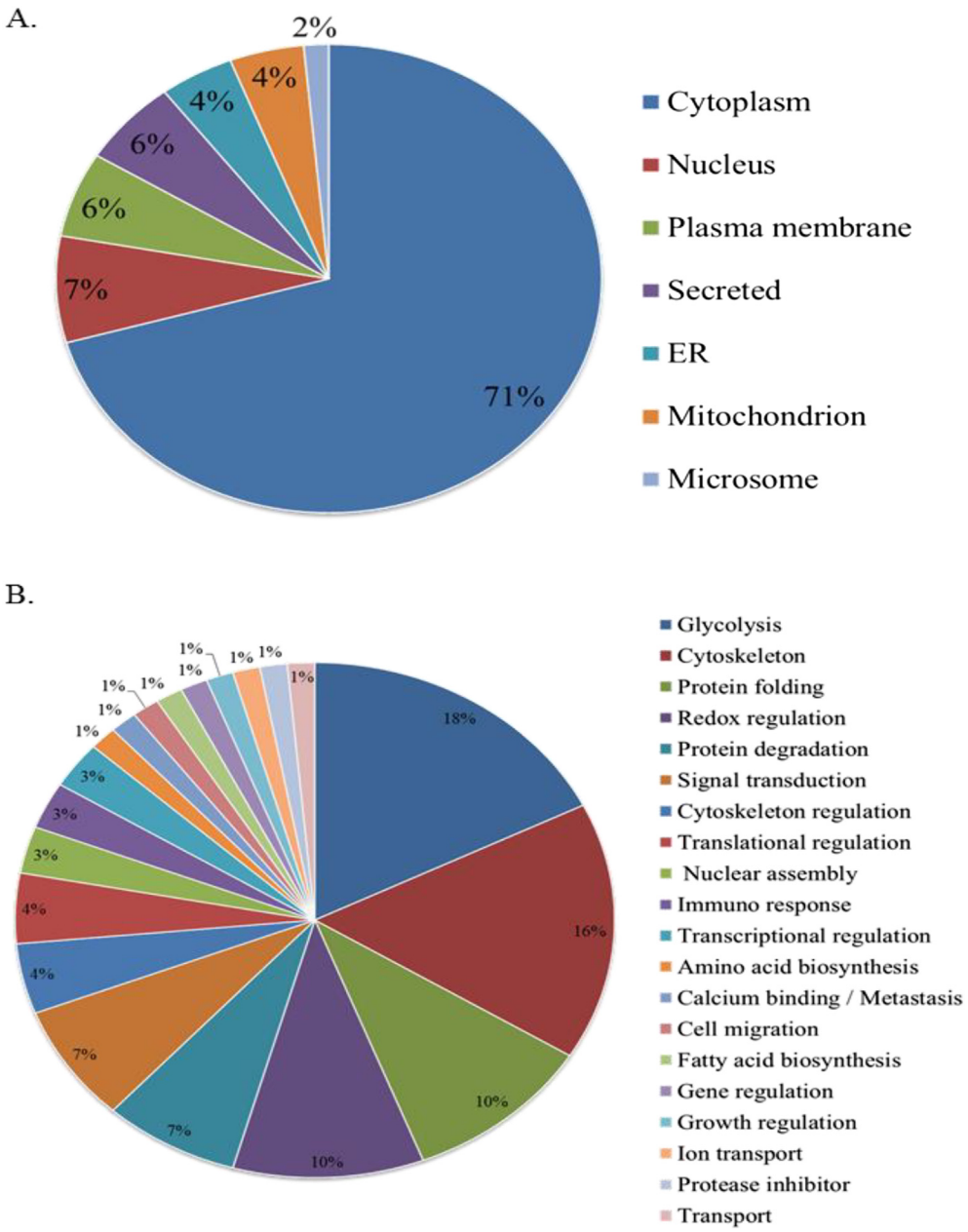

Fig. 2. Subcellular locations and functional classification of identified proteins in HeLa and HeLa-I5 cells. 68 identified proteins were classified according to their (A) subcellular locations and (B) biological functions.

cell adhesion and enhancing migratory capacity. The increased level of the EMT-inducing transcription factors such as Snail1, Snail2, Twist, ZEB1, ZEB2 can induce the expression of mesenchymal markers such as N-cadherin and Vimentin, with simultaneous decrease in the expression of epithelial marker E-cadherin [4]. During tumor progression, the occurrence of EMT allows tumor cells to acquire the capacity to invade surrounding tissue and metastasize to distant sites.

PGRMC1, a 25–28 kDa protein comprising a cytochrome b_5-like heme-binding region, belongs to the membrane-associated progesterone receptor (MAPR) protein family [5]. It is a multifunctional protein with ability to regulate cholesterol synthesis by activating the P450 protein Cyp51/lanosterol demethylase [6]. Furthermore, it is associated with DNA damage or drug mediated resistance, apoptosis suppression, cell cycle progression, and EMT induction [7,8]. PGRMC1 is highly expressed in various types of cancers, such as breast, ovarian, colon, lung, neck and oral [9]. According to a recent publication by Kabe et al., PGRMC1 forms a stable dimer structure by stacking interactions between two protruding heme molecules and this dimerization is necessary for its interaction with EGFR and cytochromes P450. They also demonstrate that the dimerization of PGRMC1 enhances cancer cell proliferation and chemoresistance [10].

Studies have shown that the function of PGRMC1 is regulated by several posttranslational modifications, including phosphorylation, ubiquitination, acetylation and SUMOylation [11]. For example, phosphorylation of PGRMC1 at Ser181 of its Casein Kinase 2 (CK2) domain is essential for its activation, whereas the phosphorylation at Y113 may promote the membrane trafficking function of PGRMC1 [12]. A differential phosphorylation pattern of PGRMC1 was also observed among estrogen receptor-positive and -negative breast cancers [13]. Above observation indicates that a detailed study of PGRMC1 is important to elucidate its biological functions and underlying mechanism in tumorigenesis.

In order to investigate cervical cancer-associated metastasis, we established an invasive HeLa-I5 cell line, which was derived from HeLa

Table 1
List of identified differentially expressed cytosolic proteins of HeLa and HeLa-I5 cells.

Master no.	SwissProt no.	Gene name	Protein name	MW	pI	No. match. Peptides	Cov. (%)	Score	Functional ontology	Subcellular location	Hela-I5/Hela	T-test	Matched peptides
1382	P61604	CH10_HUMAN	10 kDa heat shock protein, mitochondrial	10,925	8.89	12/8	58%	144	Protein folding	Mitochondrion	−1.5	0.011	M.AGQAFRK.F R.KFLPLFDR.V K.FLPLFDR.V
332	P10809	CH60_HUMAN	60 kDa heat shock protein, mitochondrial	61,187	5.7	21/12	17%	121	Protein folding	Mitochondrion	−1.43	9.80E-05	R.TVIIEQSWGSPK.V K.GANPVEIR.R K.GANPVEIRR.G
180	P11021	GRP78_HUMAN	78 kDa glucose-regulated protein	72,402	5.07	18/9	13%	78	Protein folding	ER	−2.1	1.00E-05	R.VEIIANDQGNR.I R.ITPSYVAFTPEGER.L K.VTHAVVTVPAYFNDAQR.Q
573	P11021	GRP78_HUMAN	78 kDa glucose-regulated protein	72,402	5.07	11/8	13%	96	Protein folding	ER	−1.22	0.022	R.VEIIANDQGNR.I R.ITPSYVAFTPEGER.L K.VTHAVVTVPAYFNDAQR.Q
374	Q01518	CAP1_HUMAN	Adenylyl cyclase-associated protein 1	52,325	8.24	14/8	11%	73	Signal transduction	Plasma membrane	−1.34	0.00039	M.ADMQNLVER.L + Acetyl M.ADMQNLVER.L + Acetyl R.LEAVSHTSDMHR.G
847	P15121	ALDR_HUMAN	Aldose reductase	36,230	6.51	14/7	18%	90	Redox regulation	Cytoplasm	−1.46	4.80E-05	R.LLLNNGAK.M K.SPPGQVTEAVK.V K.VAIDVGYR.H
883	P15121	ALDR_HUMAN	Aldose reductase	36,230	6.51	8/8	21%	143	Redox regulation	Cytoplasm	−1.53	0.001	R.LLLNNGAK.M K.SPPGQVTEAVK.V K.VAIDVGYR.H
1438	P06733	ENOA_HUMAN	Alpha-enolase	47,481	7.01	9/11	17%	90	Glycolysis	Cytoplasm	−1.23	0.0019	K.AVEHINK.T K.TIAPALVSK.K R.IGAEVYHNLK.N
804	P07355	ANXA2_HUMAN	Annexin A2	38,808	7.57	33/16	39%	142	Signal transduction/Ca regulation	Plasma membrane	−2.28	0.00091	K.LSLEGDHSTPPSAYGSVK.A K.AYTNFDAER.D R.QDIAFAYQR.R
873	P07355	ANXA2_HUMAN	Annexin A2	38,808	7.57	27/6	16%	62	Signal transduction/Ca regulation	Plasma membrane	1.22	0.0085	K.LSLEGDHSTPPSAYGSVK.A K.AYTNFDAER.D R.QDIAFAYQR.R
1396	P61769	B2MG_HUMAN	Beta-2-microglobulin	13,820	6.06	4/3	18%	58	Immuno response	Secreted	−1.65	5.30E-05	K.DEYACR.V R.VNHVTLSQPK.I K.IVKWDR.D
1422	P61769	B2MG_HUMAN	Beta-2-microglobulin	13,820	6.06	7/4	26%	69	Immuno response	Secreted	−1.22	0.0054	K.VEHSDLSFSK.D K.DEYACR.V R.VNHVTLSQPK.I
642	P80723	BASP1_HUMAN	Brain acid soluble protein 1	22,680	4.64	32/7	44%	82	Growth regulation	Plasma membrane	−1.75	0.00021	K.KAEGAATEEEGTPK.E K.AEGAATEEEGTPK.E K.ESEPQAAAEPAEAK.E
1252	P23528	COF1_HUMAN	Cofilin-1	18,719	8.22	8/6	28%	72	Cytoskeleton regulation	Cytoplasm	−1.22	0.0094	M.ASGVAVSDGVIK.V K.VFNDMKVR.K K.NIILEEGK.E
993	P24534	EF1B_HUMAN	Elongation factor 1-beta	24,919	4.5	10/6	24%	92	Translational regulation	Cytoplasm	−1.21	0.001	K.SPAGLQVLNDYLADK.S R.WYNHIK.S R.LAQYESK.K
1066	P20042	IF2B_HUMAN	Eukaryotic translation initiation factor 2 subunit 2	38,706	5.6	17/6	15%	62	Translational regulation	Cytoplasm	−1.25	0.029	M.SGDEMIFDPTMSK.K K.FPDEDEILEK.D K.FVMKPPQVVR.V
768	Q13347	EIF3I_HUMAN	Eukaryotic translation initiation factor 3 subunit I	36,878	5.38	9/7	20%	95	Translational regulation	Cytoplasm	1.21	0.044	-.MKPILLQGHER.S R.QINDIQLSR.D K.LFDSTTLEHQK.T
143	P15311	EZRI_HUMAN	Ezrin	69,484	5.94	10/7	15%	126	Cytoskeleton	Cytoplasm	1.2	0.0023	R.GDQPAASGDSDDDEPPPLPR.L R.DFTPAELR.R R.DFTPAELRR.F
777	P15311	EZRI_HUMAN	Ezrin	69,484	5.94	10/7	11%	88	Cytoskeleton	Cytoplasm	1.27	0.0073	R.DQWEDR.I R.IQVWHAEHR.G K.IGFPWSEIR.N
373	Q16658	FSCN1_HUMAN	Fascin	55,123	6.84	15/6	10%	78	Cytoskeleton regulation	Cytoplasm	−1.32	0.047	R.EVPGPDCR.F R.FLIVAHDDGR.W R.WSLQSEAHR.R
1330	Q01469	FABP5_HUMAN	Fatty acid-binding protein, epidermal	15,497	6.6	6/4	28%	80	Fatty acid biosynthesis	Cytoplasm	1.63	0.0015	M.ATVQQLEGR.W K.GFDEYMK.E K.ELGVGIALR.K
766	P04075	ALDOA_HUMAN	Fructose-bisphosphate aldolase A	39,851	8.3	28/14	39%	141	Glycolysis	Cytoplasm	−1.23	0.014	M.PYQYPALTPEQK.K K.ELSDIAHR.I K.GILAADESTGSIAK.R
366	P11413	G6PD_HUMAN	Glucose-6-phosphate 1-dehydrogenase	59,675	6.39	27/17	27%	191	Glycolysis	Cytoplasm	−1.56	3.30E−05	R.TQVCGILR.E R.KQSEPFFK.A K.QSEPFFK.A
1070	P09488	GSTM1_HUMAN	Glutathione S-transferase Mu 1	25,923	6.24	5/4	16%	66	Redox regulation	Cytoplasm	−1.35	0.0021	R.SQWLNEK.F K.ITQSNAILCYIAR.K K.RPWFAGNK.I
839	P04406	G3P_HUMAN	Glyceraldehyde-3-phosphate dehydrogenase	36,201	8.57	16/5	34%	145	Glycolysis	Cytoplasm	−1.32	0.00025	K.VGVNGFGR.I K.AGAHLQGGAK.R R.VIISAPSADAPMFVMGVNHEK.Y

(*continued on next page*)

Table 1 (*continued*)

Master no.	SwissProt no.	Gene name	Protein name	MW	pI	No. match. Peptides	Cov. (%)	Score	Functional ontology	Subcellular location	Hela-I5/Hela	T-test	Matched peptides
1452	P04406	G3P_HUMAN	Glyceraldehyde-3-phosphate dehydrogenase	36,201	8.57	24/9	30%	113	Glycolysis	Cytoplasm	−1.24	0.0017	K.VGVNGFGR.I K.AGAHLQGGAK.R K.IISNASCTTNCLAPLAK.V
1453	P04406	G3P_HUMAN	Glyceraldehyde-3-phosphate dehydrogenase	36,201	8.57	18/5	26%	104	Glycolysis	Cytoplasm	−1.33	0.016	K.VGVNGFGR.I K.AGAHLQGGAK.R K.IISNASCTTNCLAPLAK.V
836	P04406	G3P_HUMAN	Glyceraldehyde-3-phosphate dehydrogenase	36,201	8.57	16/5	14%	69	Glycolysis	Cytoplasm	−1.65	0.0082	K.VGVNGFGR.I K.AGAHLQGGAK.R R.GALQNIIPASTGAAK.A
242	P08107	HSP71_HUMAN	Heat shock 70 kDa protein 1A/1B	70,294	5.48	22/15	25%	166	Protein folding	ER	1.24	0.00067	K.VEIIANDQGNR.T R.TTPSYVAFTDTER.L K.NQVALNPQNTVFDAK.R
463	P31943	HNRH1_HUMAN	Heterogeneous nuclear ribonucleoprotein H	49,484	5.89	13/8	12%	80	Transcriptional regulation	Nucleus	−1.2	0.037	K.HTGPNSPDTANDGFVR.L R.GLPFGCSK.E R.THYDPPR.K
311	P61978	HNRPK_HUMAN	Heterogeneous nuclear ribonucleoprotein K	51,230	5.39	24/11	22%	96	Transcriptional regulation	Nucleus	−1.24	0.0055	R.NTDEMVELR.I R.TDYNASVSVPDSSGPER.I K.GSDFDCELR.L
429	Q09028	RBBP4_HUMAN	Histone-binding protein RBBP4	47,911	4.74	14/9	20%	112	Gene regulation	Nucleus	1.3	0.003	M.ADKEAAFDDAVEER.V K.GEFGGFGSVSGK.I K.INHEGEVNR.A
924	Q15181	IPYR_HUMAN	Inorganic pyrophosphatase	33,095	5.54	12/6	19%	75	Transport	Cytoplasm	−1.27	0.0069	M.SGFSTEER.A R.AAPFSLEYR.V R.YVANLFPYK.G
632	O75874	IDHC_HUMAN	Isocitrate dehydrogenase [NADP] cytoplasmic	46,915	6.53	8/5	11%	78	Redox regulation	Cytoplasm	−1.88	1.40E-05	R.NILGGTVFR.E R.HAYGDQYR.A R.ATDFVVPGPGK.V
579	P05783	K1C18_HUMAN	Keratin, type I cytoskeletal 18	48,029	5.34	10/8	16%	105	Cytoskeleton	Cytoplasm	−1.26	0.017	R.STFSTNYR.S R.LASYLDR.V R.AQIFANTVDNAR.I
584	P05783	K1C18_HUMAN	Keratin, type I cytoskeletal 18	48,029	5.34	25/15	26%	150	Cytoskeleton	Cytoplasm	−1.23	0.0012	R.STFSTNYR.S R.LASYLDR.V R.DWSHYFK.I
582	P05783	K1C18_HUMAN	Keratin, type I cytoskeletal 18	48,029	5.34	12/10	20%	134	Cytoskeleton	Cytoplasm	−1.65	0.00063	R.STFSTNYR.S R.LASYLDR.V K.IREHLEK.K
525	P05787	K2C8_HUMAN	Keratin, type II cytoskeletal 8	53,671	5.52	41/28	42%	282	Cytoskeleton	Cytoplasm	−1.24	0.0075	R.SYTSGPGSR.I R.ISSSSFSR.V K.FASFIDK.V
875	P07195	LDHB_HUMAN	L-lactate dehydrogenase B chain	36,900	5.17	19/14	34%	163	Glycolysis	Cytoplasm	−1.3	0.00028	K.LIAPVAEEEATVPNNK.I K.IVADKDYSVTANSK.I K.IVVVTAGVR.Q
899	P07195	LDHB_HUMAN	L-lactate dehydrogenase B chain	36,900	5.71	7/4	11%	68	Glycolysis	Cytoplasm	−1.3	0.0002	K.IVVVTAGVR.Q R.VIGSGCNLDSAR.F R.IHPVSTMVK.G
1149	O00264	PGRC1_HUMAN	Membrane-associated progesterone receptor component 1	21,772	4.56	10/7	26%	120	Signal transduction	Microsome	1.34	0.00071	R.GDQPAASGDSDDDEPPPLPR.L R.DFTPAELR.R R.DFTPAELRR.F
1074	Q13162	PRDX4_HUMAN	Peroxiredoxin-4	30,749	5.86	12/6	18%	85	Redox regulation	Cytoplasm	−1.2	0.03	K.DYGVYLEDSGHTLR.G R.GLFIIDDK.G R.QITLNDLPVGR.S
1058	P30041	PRDX6_HUMAN	Peroxiredoxin-6	25,133	6	18/9	31%	132	Redox regulation	Cytoplasm	−1.31	0.00013	R.DFTPVCTTELGR.A K.DINAYNCEEPTEK.L K.LPFPIIDDR.N
629	P00558	PGK1_HUMAN	Phosphoglycerate kinase 1	44,985	8.3	11/8	16%	102	Glycolysis	Cytoplasm	−1.2	0.0013	K.NNQITNNQR.I K.FCLDNGAK.S R.FHVEEEGKGK.D
178	P02545	LMNA_HUMAN	Prelamin-A/C	74,380	6.57	11/22	17%	102	Nuclear assembly	Nucleus	1.29	0.0047	R.SGAQASSTPLSPTR.I R.LAVYIDR.V R.SLETENAGLR.L
151	P02545	LMNA_HUMAN	Prelamin-A/C	74,380	6.57	7/4	6%	57	Nuclear assembly	Nucleus	1.28	0.011	K.NIYSEELR.E R.SSFSQHAR.T K.AQNTWGCGNSLR.T
1000	Q06323	PSME1_HUMAN	Proteasome activator complex subunit 1	28,876	5.78	13/8	30%	107	Protein degradation	Cytoplasm	−1.47	0.004	K.VDVFREDLCTK.T K.APLDIPVPDPVK.E K.APLDIPVPDPVKEK.E
1069	P60900	PSA6_HUMAN	Proteasome subunit alpha type-6	27,838	6.34	8/6	21%	92	Protein degradation	Cytoplasm	−1.24	0.011	R.LYQVEYAFK.A K.AINQGGLTSVAVR.G R.ARYEAANWK.Y
1426	P26447	S100A4_HUMAN	Protein S100-A4	11,949	5.85	12/7	36%	97	Calcium binding/ metastasis	Secreted	1.47	0.00027	K.ALDVMVSTFHK.Y K.ALDVMVSTFHK.Y R.ELPSFLGK.R

(*continued on next page*)

Table 1 (*continued*)

Master no.	SwissProt no.	Gene name	Protein name	MW	pI	No. match. Peptides	Cov. (%)	Score	Functional ontology	Subcellular location	Hela-I5/Hela	T-test	Matched peptides
276	P14618	KPYM_HUMAN	Pyruvate kinase PKM	58,470	7.96	11/6	10%	87	Glycolysis	Cytoplasm	−1.3	0.039	R.LDIDSPPITAR.N R.NTGIICTIGPASR.S K.IENHEGVR.R
1302	Q9BYM8	HOIL1_HUMAN	RanBP-type and C3HC4-type zinc finger-containing protein 1	59,359	5.47	13/5	10%	57	Protein degradation	Cytoplasm	1.2	0.017	R.AVAGGDEQVAMK.C R.NTSLNPQELQRER.Q K.DLTLQPR.G
1129	P52565	GDIR1_HUMAN	Rho GDP-dissociation inhibitor 1	23,250	5.02	9/7	17%	81	Signal transduction	Cytoplasm	−1.35	0.0051	K.YKEALLGR.V K.KQSFVLK.E K.YIQHTYR.K
539	Q5VT25	MRCKA_HUMAN	Serine/threonine-protein kinase MRCK alpha	2E+05	6.16	8/7	4%	61	Cell migration	Cytoplasm	1.3	0.024	R.QELDDAFR.Q R.EDLNKELVQASER.L K.VLLTEENK.K
664	P36952	SPB5_HUMAN	Serpin B5	42,530	5.72	17/5	14%	66	Protease inhibitor	Secreted	−1.82	3.50E-07	K.DVPFGFQTVTSDVNK.L K.LSSFYSLK.L K.IIELPFQNK.H
998	Q13126	MTAP_HUMAN	*S*-methyl-5′-thioadenosine phosphorylase	31,729	6.75	11/6	15%	66	Amino acid biosynthesis	Cytoplasm	−1.24	0.00024	R.TTMRPQSFYDGSHSCAR.G R.TTMRPQSFYDGSHSCAR.G + Oxidation (M) K.GTMVTIEGPR.F
297	P17987	TCPA_HUMAN	T-complex protein 1 subunit alpha	60,819	5.8	16/6	9%	60	Protein folding	Cytoplasm	−1.26	0.01	K.YFVEAGAMAVR.R K.YFVEAGAMAVR.R R.EQLAIAEFAR.S
206	P49368	TCPG_HUMAN	T-complex protein 1 subunit gamma	61,066	6.1	14/11	18%	123	Protein folding	Cytoplasm	1.3	0.04	R.EIQVQHPAAK.S K.MVQFEENGRK.E R.IVSRPEELR.E
1364	P10599	THIO_HUMAN	Thioredoxin	12,015	4.85	15/6	43%	92	Redox regulation	Cytoplasm	−1.22	5.30E-05	K.TAFQEALDAAGDK.L K.MIKPFFHSLSEK.Y K.MIKPFFHSLSEK.Y
1067	P60174	TPIS_HUMAN	Triosephosphate isomerase	31,057	5.65	50/14	50%	179	Glycolysis	Cytoplasm	−1.5	1.90E-05	R.KFFVGGNWK.M K.FFVGGNWK.M K.VPADTEVVCAPPTAYIDFAR.Q
773	P07951	TPM2_HUMAN	Tropomyosin beta chain	32,945	4.66	30/10	23%	93	Cytoskeleton	Cytoplasm	−1.24	0.018	K.LDKENAIDR.A K.KATDAEADVASLNR.R K.ATDAEADVASLNR.R
473	P07437	TBB5_HUMAN	Tubulin beta chain	50,095	4.78	15/9	15%	102	Cytoskeleton	Cytoplasm	−1.22	0.0034	K.IREEYPDR.I R.IMNTFSVVPSPK.V R.FPGQLNADLR.K
324	Q96FW1	OTUB1_HUMAN	Ubiquitin thioesterase OTUB1	31,493	4.85	6/4	16%	76	Protein degradation	Cytoplasm	1.26	0.0014	R.IQQEIAVQNPLVSER.L K.TRPDGNCFYR.A R.LLTSGYLQR.E
1331	P05161	ISG15_HUMAN	Ubiquitin-like protein ISG15	17,933	6.24	7/5	27%	89	Protein degradation	Cytoplasm	−2.15	0.048	M.GWDLTVK.M K.IGVHAFQQR.L R.LAVHPSGVALQDR.V
386	P08670	VIME_HUMAN	Vimentin	53,676	5.06	52/26	47%	232	Cytoskeleton	Cytoplasm	1.24	0.0024	R.MFGGPGTASRPSSSR.S R.SYVTTSTR.T R.TYSLGSALRPSTSR.S
387	P08670	VIME_HUMAN	Vimentin	53,676	5.06	23/14	30%	149	Cytoskeleton	Cytoplasm	1.27	0.0015	R.MFGGPGTASRPSSSR.S R.SYVTTSTR.T R.TYSLGSALRPSTSR.S
403	P08670	VIME_HUMAN	Vimentin	53,676	5.06	26/14	30%	152	Cytoskeleton	Cytoplasm	1.31	0.0019	R.SVSSSSYR.R R.SVSSSSYRR.M R.MFGGPGTASRPSSSR.S
1007	P21796	VDAC1_HUMAN	Voltage-dependent anion-selective channel protein 1	30,868	8.62	16/6	19%	79	Ion transport	Mitochondrion	−1.56	0.0026	M.AVPPTYADLGK.S K.GYGFGLIK.L K.LTFDSSFSPNTGK.K
289	O75083	WDR1_HUMAN	WD repeat-containing protein 1	66,836	6.17	20/8	9%	62	Cytoskeleton regulation	Cytoplasm	−1.26	0.00034	K.VFASLPQVER.G K.YEYQPFAGK.I R.IAVVGEGR.E

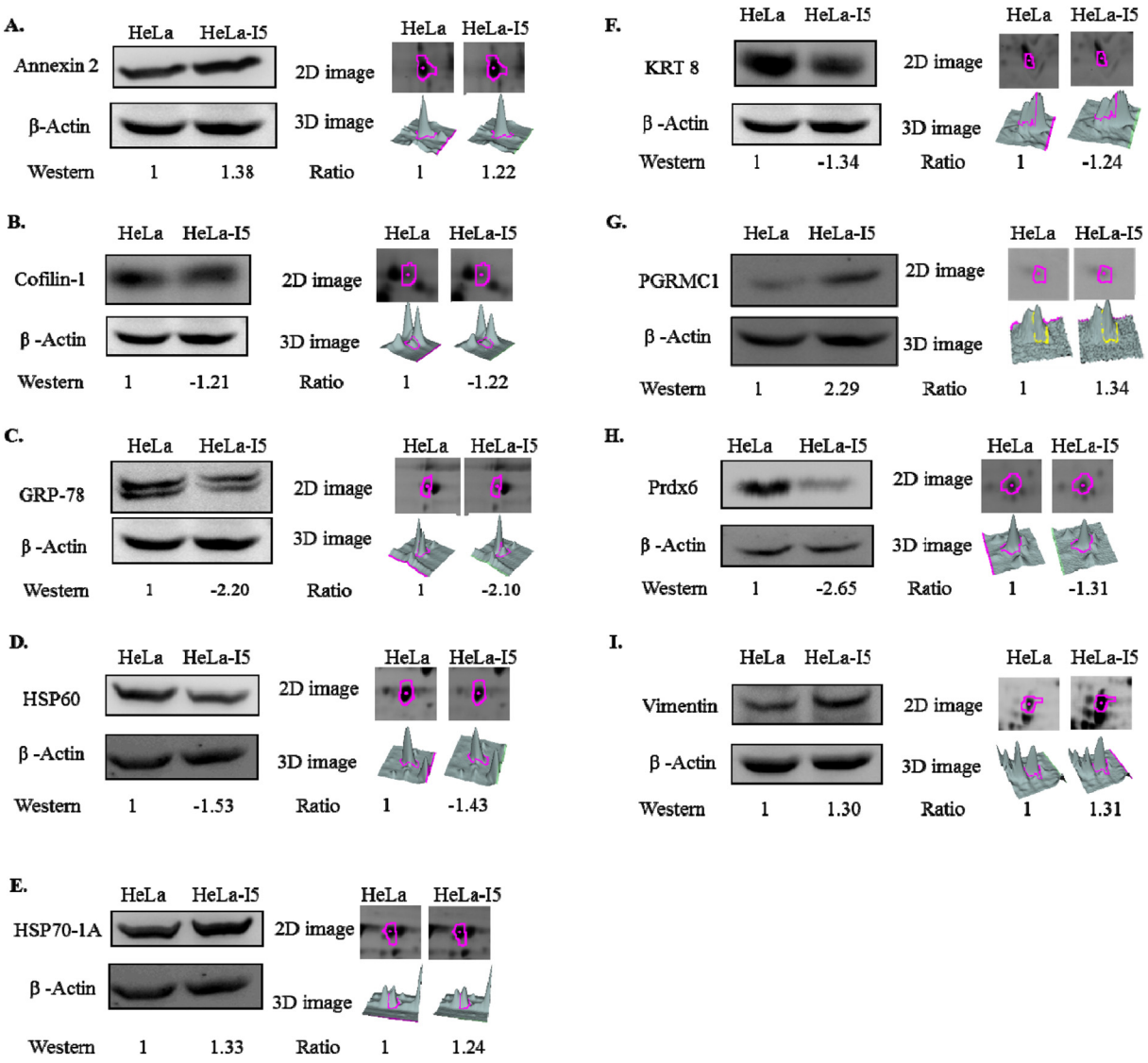

Fig. 3. Validation of identified proteins between HeLa and HeLa-I5 cells by Western blot analysis. Left panels showed the representative Western blot images. Right panels showed the protein 2D-DIGE maps (top), three-dimensional spot images (middle) and 2D ratio (bottom). (A) Annexin 2 (B) Cofilin-1 (C) GRP-78 (D) HSP60 (E) HSP70-1A (F) KRT 8 (G) PGRMC1 (H) Prdx6 (I) Vimentin.

cell line after passing it through transwell invasion assays, resulting in cells with high migratory and proliferation abilities. Next, the proteomic analysis was performed in HeLa and invasive HeLa-I5 cells and 68 differentially expressed proteins were identified. Out of 68, a metastatic-related protein, PGRMC1 was selected as a candidate protein to understand its role in cervical cancer metastasis. To verify the role of PGRMC1 in cervical cancer metastasis, invasive CaSki-I5 and ME-180-I5 were also established from their respective parental CaSki and ME-180 cells, similar to HeLa-I5 cells. With this study, we aim to provide an effective diagnostic and therapeutic target for metastatic cervical cancer.

2. Materials and methods

2.1. Cell lines and cell culture

2.1.1. Cell lines and subculture

The human cervical adenocarcinoma cancer cell line (HeLa) and the human cervical epidermoid carcinoma cell lines (ME-180 and CaSki) were provided by Dr. Yung–Jen Chuang (NTHU, Taiwan). HeLa were cultured in Dulbecco's Modified Eagle Medium (DMEM) and ME-180 and CaSki were cultured in Roswell Park Memorial Institute −1640 medium (RPMI-1640) supplemented with 10% cosmic calf serum (CCS), 100 IU/ml penicillin, and 100 μg/ml streptomycin (all from Gibco-Invitrogen Corp., UK) at 37 °C in a humidified atmosphere of 5% CO_2.

2.1.2. Cell selected by transwell invasion assay

HeLa-I5, Ca Ski-I5 and ME-180-I5 cells were selected by transwell invasion assay. Transwell 6.5 mm diameter inserts with 8.0 μm pore size (Corning Incorporated) were coated with Matrigel™ (BD Biosciences). Matrigel™ was diluted 1: 3 with chilled serum-free medium just prior to coating. 50 μl of the chilled diluted Matrigel was placed directly onto the center of transwell inserts and then placed the plate into the incubator at 37 °C for 60 min to allow gelling. 2×10^5 cells in 100 μl serum-free medium were added to the inserts and 700 μl complete medium were added to the lower chamber as attractant for invading cells. The plate was incubated at for 24 h at 37 °C in a humidified atmosphere of 5% CO_2. The non-invading cells remaining on the upper surface of the inserts were removed by a cotton swab. The inserts were washed by PBS three times and the invading cells on the lower surface of the inserts were trypsinized and resuspended in complete

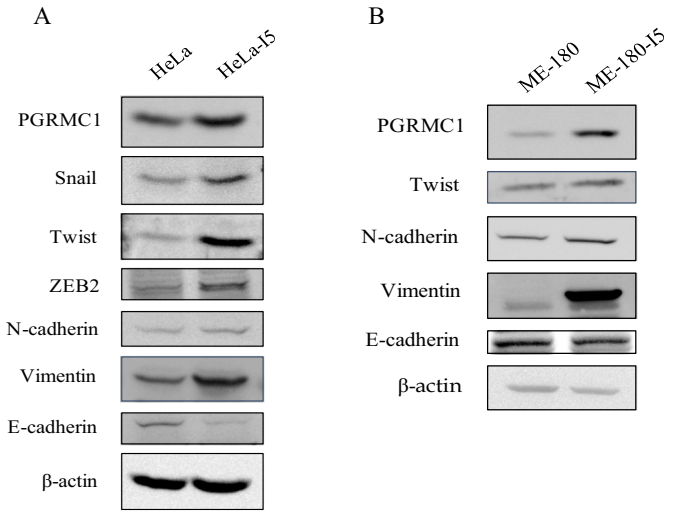

Fig. 4. Identify the expression level of EMT markers and PGRMC1 in invasive cervical cancer cell lines. The expression level of EMT markers and PGRMC1 were identified by Western blot analysis. β-Actin was used as loading control. (A) Western blot analysis of EMT markers and PGRMC1 expression in HeLa and HeLa-I5 cells. (B) Western blot analysis of EMT markers and PGRMC1 expression in ME-180 and ME-180-I5 cells.

medium.

2.2. Western blot analysis

Cells were washed by 0.5 × PBS three times and lysed by Nonidet P-40 (NP40) lysis buffer containing 4 μl/ml phosphotase inhibitor (Sigma-Aldrich) and 1 μl/ml protease inhibitor (A.G. Scientific, Inc.) on ice. Samples were pelleted by centrifugation at 13,000 rpm for 30 min at 4 °C. Protein concentrations were measured using a Bradford Protein Assay (Bio Rad). The lysates were mixed with NP40 lysis buffer and 5 × Laemmli sample buffer (60 mM Tris-HCl pH 6.8, 10% (*v*/v) glycerol, 5% β-mercaptoethanol, 2% (*w*/*v*) SDS, 0.01% (w/v) bromophenol blue) boiled at 95 °C for 10 min. The same amount samples of different conditions were electrophoresed through 12% SDS-PAGE and transferred to polyvinylidene fluoride (PVDF) membranes (Millipore, Billerica, MA, USA). The PVDF membranes were blocked with 5% non-fat milk in 1 × Tris-buffered saline with Tween 20 (1 × TBST) washing buffer, probed with primary antibody overnight at 4 °C and followed by incubation with the horseradish peroxidase (HRP)-conjugated secondary antibodies (Jackson immune Research, Inc.) for 1 h. The immunoreactive bands on the blots were detected by an enhanced chemiluminescence (ECL) kit (Visual Protein Biotechnology, Inc.) and scanned by LAS 4000 (GE Healthcare).

2.3. Transwell migration assay

Cells at a density of 5×10^4 cells in 100 μl serum-free medium were plated into the transwell inserts and 700 μl complete medium which contained 10% CCS were added to the lower chamber. The transwell plate was incubated at 37 °C in a humidified atmosphere of 5% CO_2. After 20–22 h of incubation, the cells on the upper surface of the inserts were removed by a cotton swab. The migrated cells were fixed with 4% paraformaldehyde solution (PFA) (USB Corporation, Cleveland, OH, USA) for 25 min and stained with crystal violet for 5 min. Then, the crystal violet was dissolved in ethanol/acetic acid solution and quantified.

2.4. Cell cycle analysis by flow cytometry

For cell cycle analysis, 1×10^6 cells were collected by trypsinization

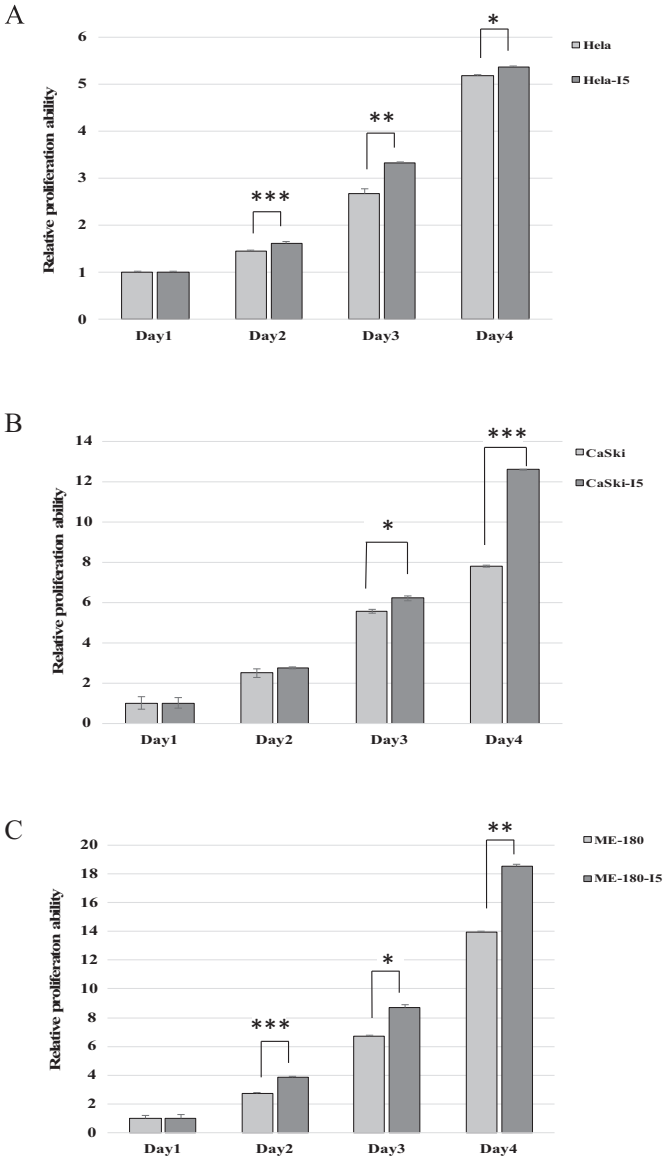

Fig. 5. Proliferation abilities of the invasive cervical cancer cell lines compared to the parental cervical cancer cell lines. MTT-based cell proliferation assays were performed to observe the cell proliferation rate from Day 1 to Day 4. The values of relative proliferation ability were normalized to Day 1 respectively. (A) Relative proliferation ability of HeLa-I5 cells compared to HeLa cells. (B) Relative proliferation ability of CaSki-I5 cells compared to CaSki cells. (C) Relative proliferation ability of ME-180-I5 cells compared to ME-180 cells. Error bars denote mean ± SEM. *$p < 0.05$, **$p < 0.01$, ***$p < 0.001$.

and washed with PBS twice, fixed in 70% alcohol at 4 °C for 30 min, and washed with PBS again. The cells were then stained with 500 μl of propidium iodide (PI) buffer (50 μg/ml PI dye and 100 μg/ml RNase in 1 × PBS), incubated in a darkroom at 4 °C for 30 min, and evaluated using a BD Accuri flow cytometer (BD Biosciences, San Jose, CA).

2.5. MTT cell proliferation assay

Prepare 3000 cells in 200 μl complete medium into 96-well plates. The plates were incubated for 4–6 days at 37 °C in a humidified atmosphere of 5% CO_2. Cells were treated with MTT (USB Corporation, Cleveland, OH, USA) solution (1 mg/ml) 100 μl per well at 37 °C for 4 h every 24 h. After 4 h incubation, 100 μl dimethyl sulfoxide (DMSO) (TEDIA, Shanghai) was added per well to dissolve the insoluble formazan. Measure the optical density (OD) values at 570 nm by ELISA

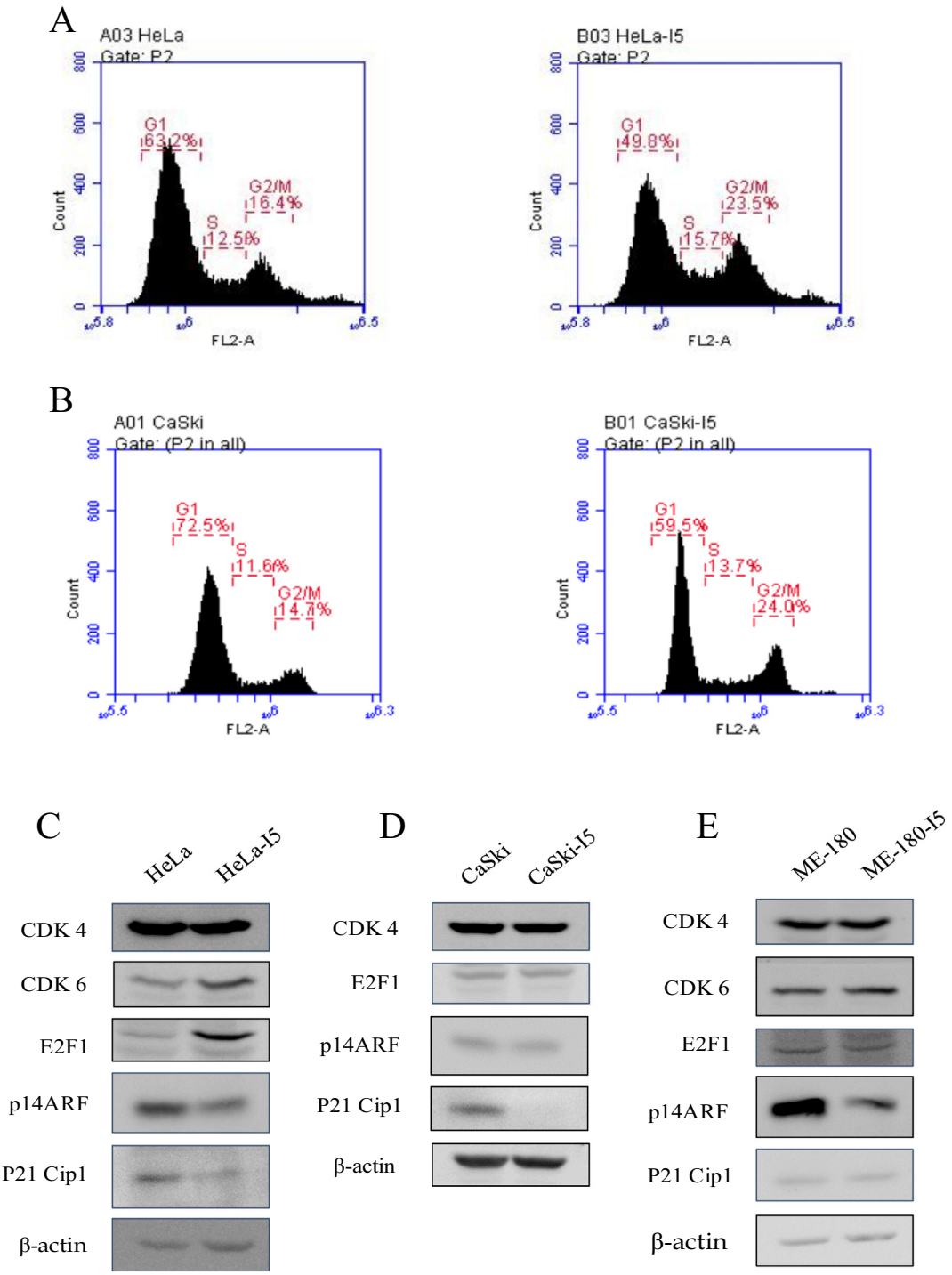

Fig. 6. Reveal cell cycle regulation in invasive cervical cancer cell lines compared to the parental cervical cancer cell lines. Cell cycle analysis by flow cytometer. Cells were stained with PI buffer, incubated in a darkroom at 4 °C for 30 min, and evaluated by flow cytometer to analyze DNA content. The percentage of cells in the G1, S, and G2/M phases were displayed on the FL2-A fluorescent channel of the flow cytometer. (A) Representative plots of cell cycle analysis in HeLa and HeLa-I5 cells. (B) Representative plots of cell cycle analysis in CaSki and CaSki-I5 cells. (C) Western blot analysis of cell cycle regulatory proteins in HeLa and HeLa-I5 cells. β-Actin was used as loading control. (D) Western blot analysis of cell cycle regulatory proteins in CaSki and CaSki-I5 cells. β-Actin was used as loading control. (E) Western blot analysis of cell cycle regulatory proteins in ME-180 and ME-180-I5 cells. β-Actin was used as loading control.

reader.

2.6. siRNA transfection

Specific knockdown was achieved by transfecting cells with siRNAs against PGRMC1. The targeting sequences 5′-AAU UUG CGG CCU UUG GUC ACA UCG A-3′ and 5′-AGU GAA CUG AGA CUC CCA GUC ACU C-3′ against PGRMC1 were synthesized by Invitrogen (Invitrogen). Cells were transfected with 25 nM siRNA using Lipofectamine® LTX (Invitrogen) according to the manufacturer's instructions in serum free medium for 4 h followed by recovering in complete medium which contained 10% CCS for 24 h and repeated the steps twice.

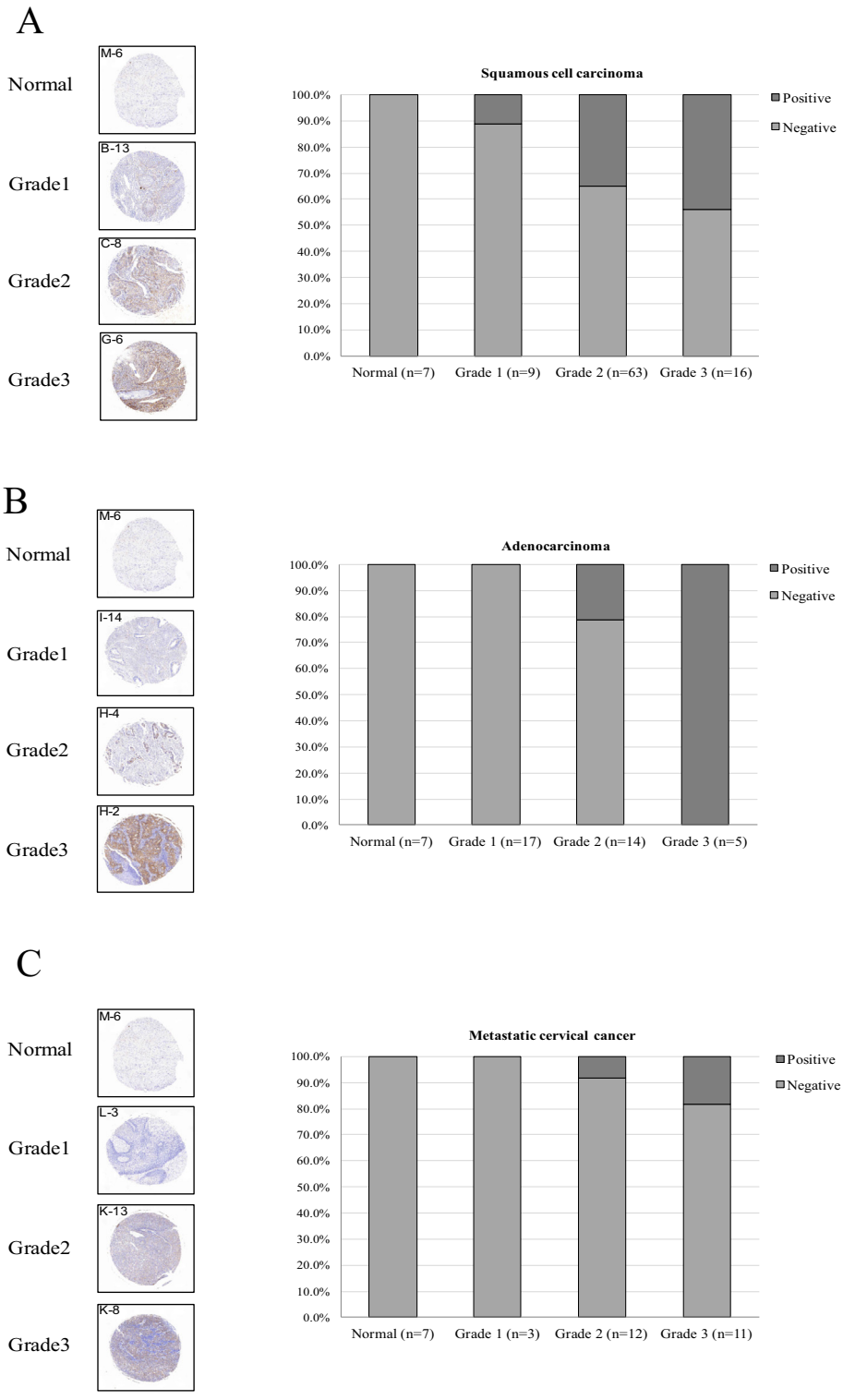

Fig. 7. PGRMC1 expression in tissue array specimens of cervical cancer. Clinical cervical cancer specimens on a tissue microarray were stained for PGRMC1in different cancer types by tumor grade. Data was obtained from 58 cases of cervical cancer and 9 cases of normal tissue. Each case had triplicated cores. (A) Representative tissue specimen images of squamous cell carcinoma with immunohistochemical staining for PGRMC1 by tumor grade and the quantified bar graphs presented the percentage of negative and positive staining for PGRMC1 of grade 1, 2, and 3 compared to normal cervix tissues. (B) Representative tissue specimen images of cervical adenocarcinoma with immunohistochemical staining for PGRMC1 by tumor grade and the quantified bar graphs. (C) Representative tissue specimen images of metastatic cervical cancer with immunohistochemical staining for PGRMC1 by tumor grade and the quantified bar graphs.

3. Results

3.1. Comparison of proteomics data between the invasive and the parental cervical cancer cells

In order to elucidate the mechanism of cervical cancer metastasis, we established an invasive cervical cancer cell line HeLa-I5, which was derived from HeLa cells by selecting the cells, which underwent the transwell invasion assay. Next, we performed two-dimensional differential in-gel electrophoresis (2D-DIGE) and matrix-assisted laser desorption ionization time-of-flight mass spectrometry (MALDI-TOF MS/MS) to identify the differentially expressed proteins among HeLa and HeLa-I5 cells. The 2D-DIGE images of differentially expressed protein in HeLa and HeLa-I5 cells were profiled by Ettan DIGE Imager, followed by analysis using DeCyder software version 7.0. Dust and background were filtered out on the basis of spot slope, volume, and area. Total 122 protein spots were found to be differentially expressed within the average ratio of "≥ 1.2-to-≤ -1.2 fold", at $p \leq 0.05$ (*t*-test),

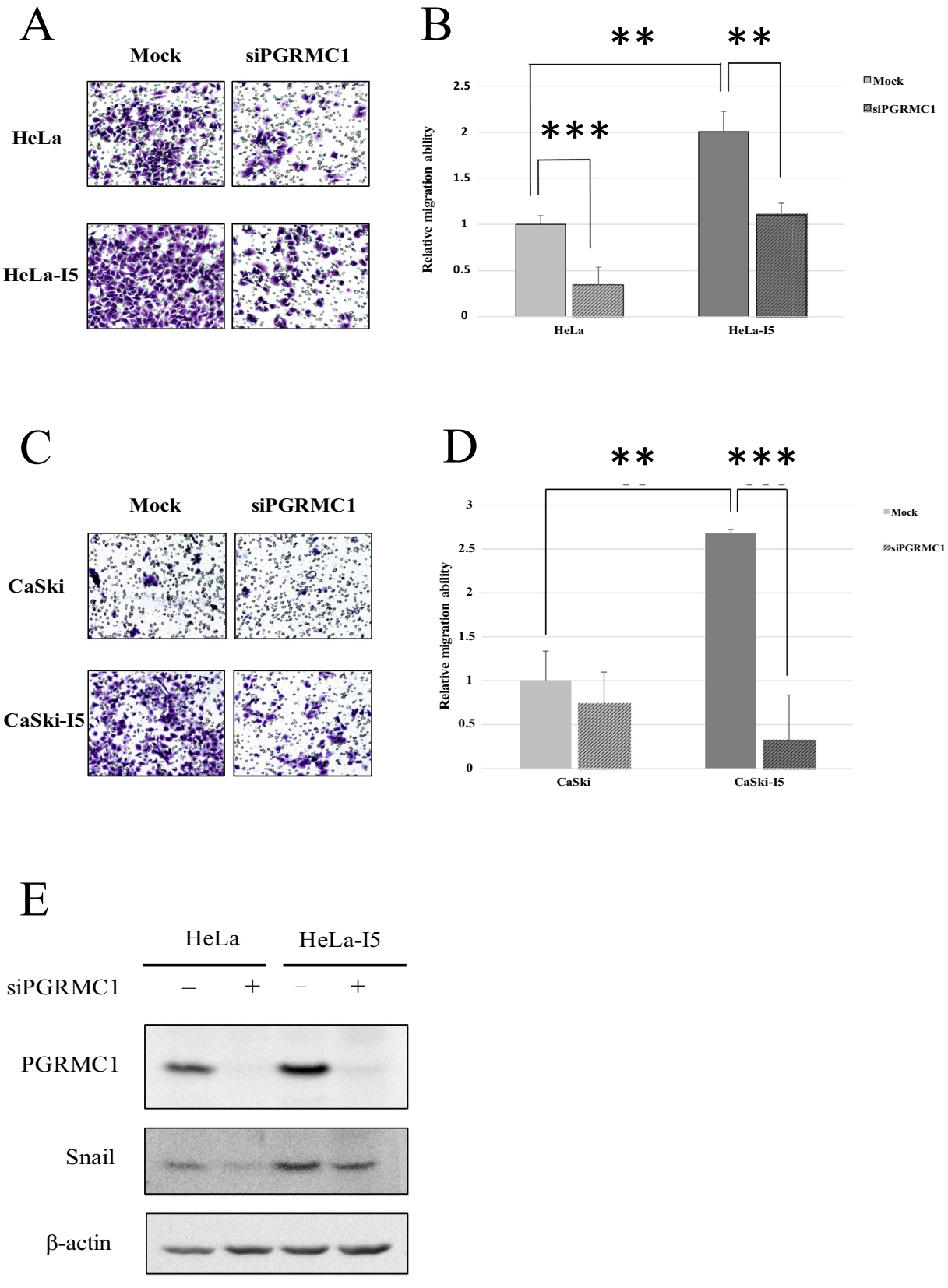

(caption on next page)

out of which 119 spots were picked for further identification (Fig. 1A–C). Next, the spots were digested by trypsin to cleave protein chain at the carboxyl side of arginine, followed by peptide mass fingerprint (PMF) analysis using MALDI-TOF MS/MS. Finally, 68 proteins were identified and classified according to their subcellular localization and biological functions (Fig. 2A and B and Table 1). Up to 70% of the total proteins were cytosolic having biological roles in glycolysis, protein folding, redox regulation protein degradation and cytoskeleton-

Fig. 8. siRNA-mediated PGRMC1 knockdown inhibit the migration ability in cervical cancer cell lines. HeLa, HeLa-I5, CaSki and CaSki-I5 cells were transfected with 25 nM siRNAs against PGRMC1 for 4 h followed by recovering in complete medium for 24 h. The migration abilities were monitored by transwell migration assays. (A) Representative images of transwell migration assay were viewed under microscope at 20× magnification showed the HeLa-Mock, HeLa-siPFFRMC1, HeLa-I5-Mock and HeLa-I5-siPGRMC1 cells that migrated through the filters of transwell inserts. (B) The migrated cells were quantified by ELISA reader. The value of the relative migration ability was normalized to the HeLa-Mock cells. Both HeLa-siPGRMC1 cells and HeLa-I5-siPGRMC1 cells showed significantly lowered migration ability than HeLa-Mock cells and HeLa-I5-Mock cells respectively. Error bars denote mean ± SEM. $^{**}p < 0.01$, $^{***}p < 0.001$. (C, D) Representative images and quantitative analysis of transwell migration assay for CaSki-Mock, CaSki-siPGRMC1, CaSki-I5-Mock and CaSki-I5-siPGRMC1 cells. CaSki-I5-siPGRMC1 cells showed significantly lowered migration ability than CaSki-I5-Mock cells. Error bars denote mean ± SEM. $^{**}p < 0.01$, $^{***}p < 0.001$. (E) Western blot analysis of Snail and PGRMC1 expression in siRNA-mediated PGRMC1 knockdown HeLa and HeLa-I5 cells. β-Actin was used as loading control.

organization. Furthermore, Western blot analyses were performed to validate the differential expression of identified proteins between HeLa and HeLa-I5 cells (Fig. 3A–I).

Among selected proteins, PGRMC1 was found to be up-regulated in invasive HeLa-I5 cells as compared to HeLa cells (Fig. 3G). Studies have shown an up-regulation in the protein and mRNA level of PGRMC1 in a variety of tumors including lung, thyroid, colon, breast and so on. The upregulation of PGRMC1 is correlated to cancer progression, chemotherapy resistance and cancer metastasis. However, the correlation between PGRMC1 and cervical cancer metastasis has not been studied thoroughly. In present study, PGRMC1 was selected as a potential candidate for further investigation of its role in cervical cancer metastasis.

3.2. Establishment of invasive cervical cancer cell lines

To demonstrate the mechanism of cervical cancer metastasis, we established two more invasive cervical cancer cell lines, CaSki-I5 and ME-180-I5. These invasive cell lines were also derived from parental CaSki and ME-180 lines by the selecting the cells after transwell invasion assays. The transwell migration assays were also performed to confirm the differential migration abilities of parental and the invasive cervical cancer cell lines. HeLa-I5 cells showed around 2-fold increase in migration than that of HeLa cells, whereas CaSki-I5 and ME-180-I5 cells respectively showed 3.1- and 8.6-fold increase in migration than that of their parental cells (data not shown).

3.3. Correlation between the expression level of EMT markers and PGRMC1 in invasive cervical cancer cell lines

After confirming the higher migration ability of HeLa-I5, CaSki-I5 and ME-180-I5 cells, we wondered if the parental-to-invasive cell type transition is because of epithelial-mesenchymal transition of cells. To test this, the expression level of EMT markers such as SIP, Snail, Twist, N-cadherin, Vimentin and E-cadherin in HeLa, HeLa-I5, ME-180 and ME-180-I5 lines were examined by Western blot. Differential expressions of the markers were observed between parental and invasive cell lines. In Hela-I5 cells, the expression of E-cadherin was decreased with concomitant increase in ZEB2, Snail, Twist, N-cadherin, and Vimentin levels (Fig. 4A). Similarly, in ME-180-I5 cells, expression of Twist, N-cadherin, and Vimentin were high accompanied by low levels of E-cadherin (Fig. 4B). In summary, all three invasive cell lines were found to have EMT characteristic. In addition to the expression of EMT markers, the expression of PGRMC1 was also upregulated in invasive cell lines as compared to their parental cells (Fig. 4A and B).

3.4. Comparison of cell viability between invasive and parental cervical cancer cell lines

Further, the MTT assays were performed for 4 days to evaluate the difference in cell viability among invasive (HeLa-I5, CaSki-I5 and ME-180-I5) and their respective parental cell lines. The relative viability was calculated by normalizing the data to viability of the cells at Day 1. The viability rate was significantly higher in HeLa-I5 cells as compared to HeLa cells (Fig. 5A). The same pattern was also observed in CaSki-I5 cells (Fig. 5B) and ME-180-I5 cells (Fig. 5C). The data indicated that invasive cell lines exhibited higher viability than their respective parental lines.

3.5. Analysis of cell cycle regulation in invasive cervical cancer cell lines

Next, we performed cell cycle analysis using flow cytometry to compare the cell cycle regulation between HeLa-I5 and HeLa cells. The cells were stained with propidium iodide (PI) to analyze DNA content. The cell cycle analysis plot showed a decreased percentage of cells in G1 phase (49.8%) with simultaneous increase in S (15.7%) and G2/M (23.5%) phases in HeLa-I5 cells as compared to HeLa cells (G1 phase: 63.2%, S phase: 12.5%, G2/M phase: 16.4%) (Fig. 6A). A similar pattern was also observed between CaSki and CaSki-I5 cells. CaSki-I5 cells showed a decreased percentage of cells in G1 phase (57.5%) with an increase in S (13.7%) and G2/M (24%) phases as compared to CaSki cells (G1 phase: 72.5%, S phase: 11.6%, G2/M phase: 14.7%) (Fig. 6B). Furthermore, the expression of cell cycle regulatory proteins was examined by Western blot. The expression level of CDK6 and E2F1 were up-regulated, whereas the levels of p14ARF and p21Cip1 were down-regulated in HeLa-I5 cells as compared to HeLa cells (Fig. 6C). Similar results were observed in CaSki-I5 and ME-180-I5 cells (Fig. 6D and E), where the expression of CDK6 was up-regulated with simultaneous down-regulation in p14ARF and p21Cip1 expressions. CDK4 was not differentially expressed between invasive and their respective parental cell lines. CDK6, E2F1, p14ARF and p21Cip1 proteins play important role in regulating cell cycle progression especially in G1 phase. This suggests that the increased proliferation rate in invasive cervical cancer cells might be due to the involvement of G1 phase regulatory proteins.

3.6. The expression of PGRMC1 differed between various grades of cervical cancer

We performed immunohistochemistry (IHC) of cervical cancer tissue array (Biomax, USA) to examine the PGRMC1 expression level in different grade of cervical cancer. The specimens were stained with PGRMC1 antibody (Abcam # ab80941, USA), followed by quantification of expression on the basis of staining intensity and the percentage of positively stained cells. The staining intensity was scored as either non-existent (0), weak (1), moderate (2) or strong (3), whereas the number of stained cells was scored as either no cells stained (0), < 10% (1), 10–50% (2), 50–80% (3) or > 80% cells stained (4). The final score was calculated by multiplying these two variables. A score of 0–5 was considered negative indicating no over-expression of PGRMC1, whereas a score higher than 6 was considered positive indicating PGRMC1 overexpression [14]. he data revealed that The all the subtypes of cervical cancer, squamous cell carcinoma (Fig. 7A), cervical adenocarcinoma (Fig. 7B) and metastatic cervical cancer (Fig. 7C), PGRMC1 was over-expressed in grade 3 as compared to normal, grade 1 and grade 2 tumors.

3.7. siRNA-mediated knockdown of PGRMC1 inhibited the migration ability of cervical cancer cells

According to our proteomics and Western blot data, PGRMC1 expression was found to be up-regulated in HeLa-I5, CaSki-I5 and ME-180-I5 cells as compared to their respective parental lines. Studies have

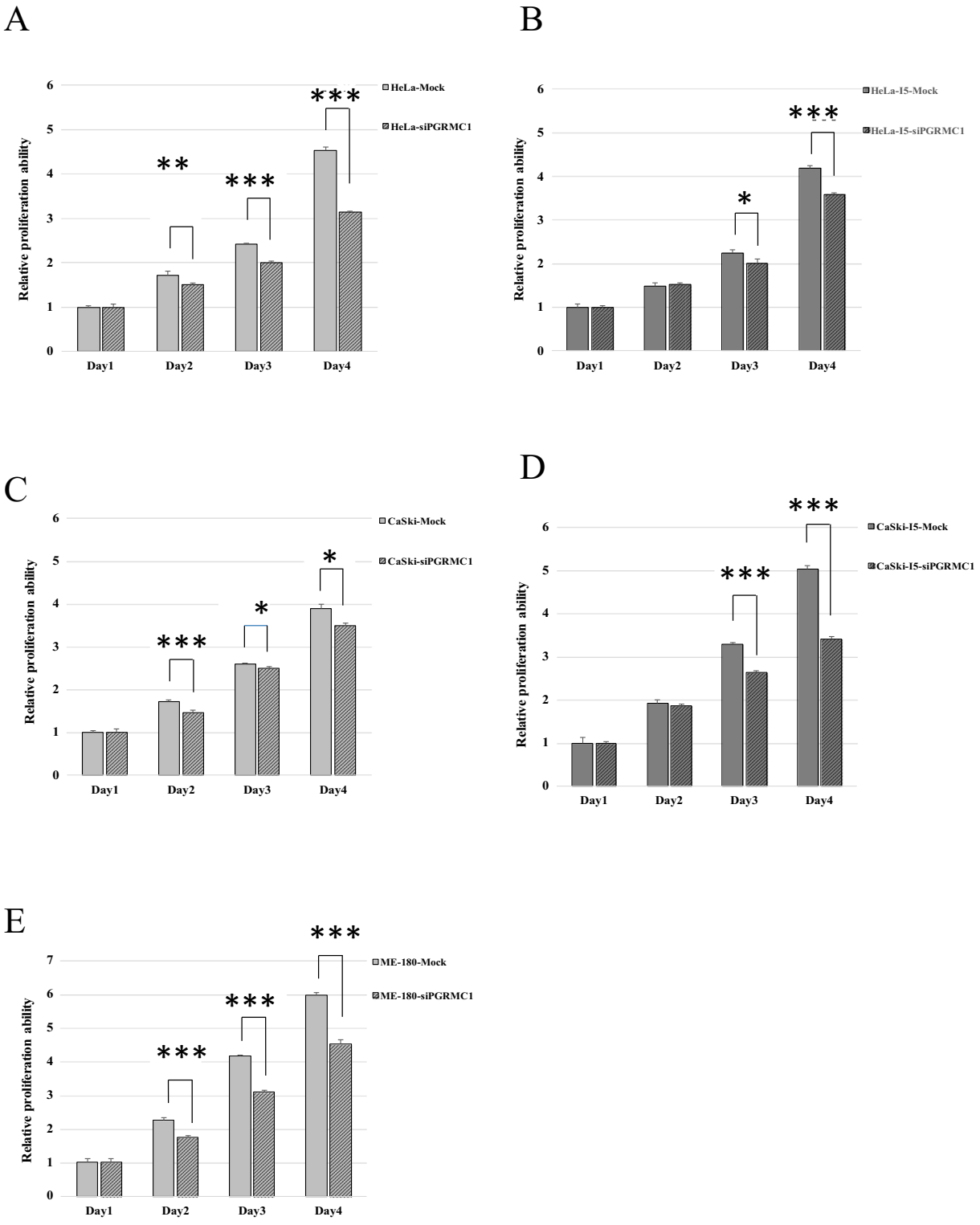

Fig. 9. siRNA-mediated PGRMC1 knockdown inhibit the proliferation ability in cervical cancer cell lines. HeLa, HeLa-I5, CaSki, CaSki-I5 and ME-180 cells were transfected with 25 nM siRNAs against PGRMC1 for 4 h followed by recovering in complete medium for 24 h. MTT-based cell proliferation assays were performed to observe the cell proliferation rate from Day 1 to Day 4. The values of relative proliferation ability were normalized to Day 1 respectively. (A) Relative proliferation ability of HeLa-siPGRMC1 cells compared to HeLa-Mock cells. (B) Relative proliferation ability of HeLa-I5-siPGRMC1 cells compared to HeLa-I5-Mock cells. (C) Relative proliferation ability of CaSki-siPGRMC1 cells compared to CaSki-Mock cells. (D) Relative proliferation ability of CaSki-I5-siPGRMC1 cells compared to CaSki-I5-Mock cells. (E) Relative proliferation ability of ME-180-siPGRMC1 cells compared to ME-180-Mock cells. Error bars denote mean ± SEM. $*p < 0.05$, $**p < 0.01$, $***p < 0.001$.

shown that PGRMC1 is over-expressed in a various cancers such as breast, ovarian and lung cancers and promotes cancer cell proliferation, chemotherapy resistance, angiogenesis and metastasis. It led us to speculate a causative role of PGRMC1 in cervical cancer progression also. To confirm this, firstly a siRNA-mediated PGRMC1 knockdown was performed and migration ability of cervical cancer cells was

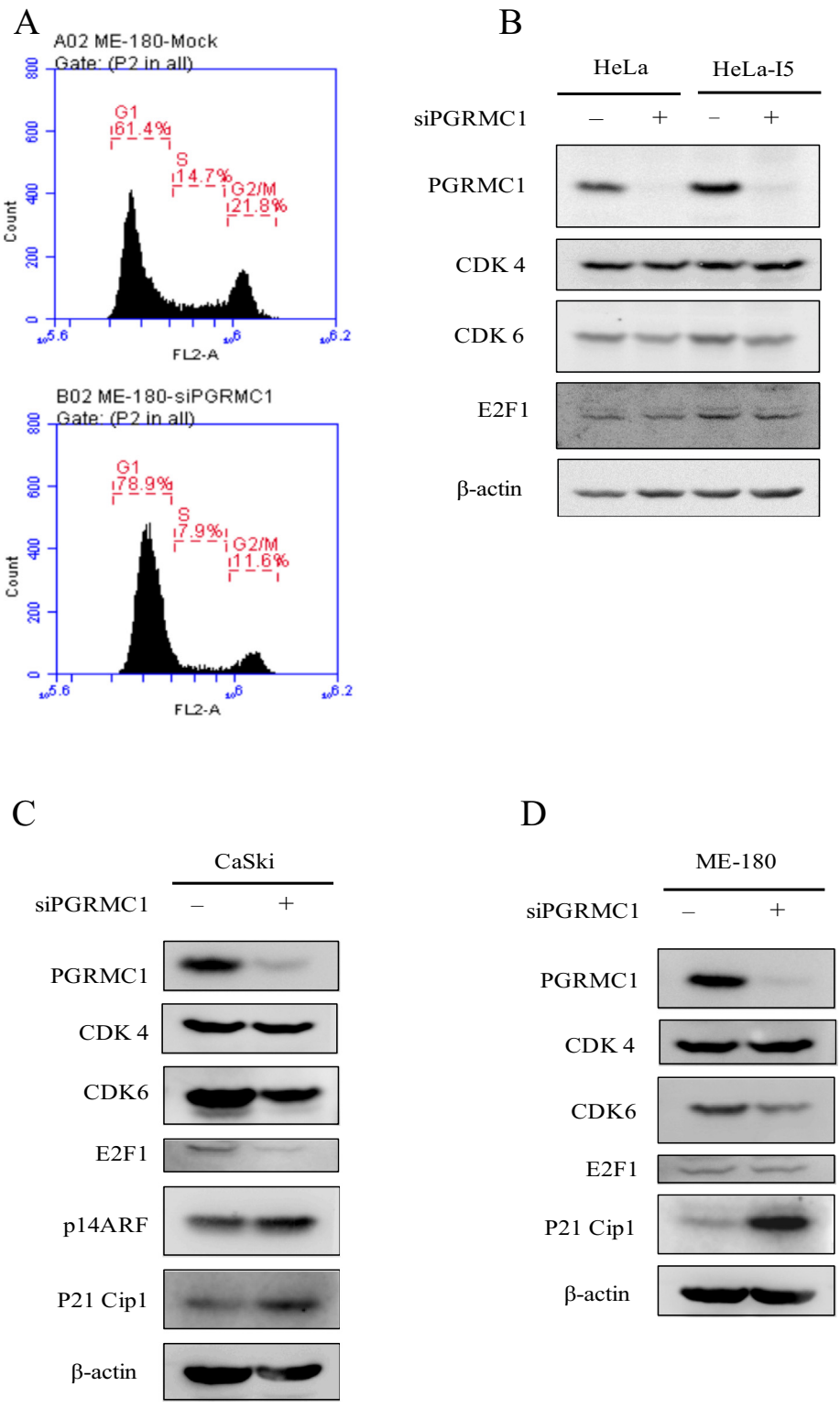

Fig. 10. Investigate cell cycle regulation in siRNA-mediated PGRMC1 knockdown cell lines. (A) Representative plots of cell cycle analysis by flow cytometer. ME-180 and ME-180-siPGRMC1 cells were stained with PI buffer, incubated in a darkroom at 4 °C for 30 min, and evaluated by flow cytometer to analyze DNA content. The percentage of cells in the G1, S, and G2/M phases were displayed on the FL2-A fluorescent channel of the flow cytometer. (B, C, D) Western blot analysis of cell cycle regulatory proteins. The expression of cell cycle regulatory proteins was differentially expressed in siRNA-mediated PGRMC1 knockdown cell lines compared to si-Mock cell lines. β-Actin was used as loading control.

estimated. Both HeLa-I5 and HeLa cells showed significantly reduced migration ability after PGRMC1 knockdown (Fig. 8A and B). A similar result also observed in CaSki-I5-Mock and CaSki-I5-siPGRMC1 cells (Fig. 8C and D). We further examined the expression level of EMT markers in siPGRMC1 knockdown cells by Western blot analysis. The data revealed a significantly decreased expression of Snail in HeLa-siPGRMC1 cells and HeLa-I5-siPGRMC1 (Fig. 8E) as compared to respective mock cells, suggesting that PGRMC1 might promote cervical cancer cell migration via regulating EMT proteins such as Snail.

3.8. siRNA-mediated PGRMC1 knockdown reduce cell proliferation of cervical cancer cell lines

To determine the role of PGRMC1 on cellular proliferation, siRNA-mediated PGRMC1 knockdown was performed, followed by MTT-based cell proliferation assay. The relative proliferation ability was represented as a value normalized to the viability at Day 1. A significant inhibition of cell growth was observed in the cervical cancer cells transfected with siPGRMC1. The proliferation ability was significantly

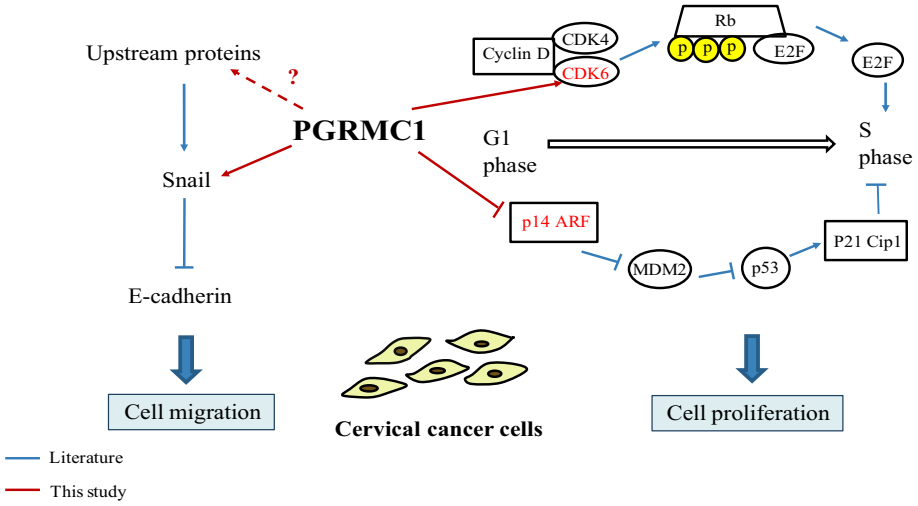

Fig. 11. Schematic depicting the possible mechanism of PGRMC1 on cervical cancer metastasis. PGRMC1 might promote cancer metastasis via increasing the expression of Snail which is an EMT transcription factor and promote cancer cell progression through modulating the cell cycle G1/S phase regulatory proteins.

decreased in HeLa-siPGRMC1 cells compared to HeLa-Mock cells (Fig. 9A). A similar phenomenon was also observed in HeLa-I5-siPGRMC1, CaSki-siPGRMC1, CaSki-I5-siPGRMC1, and ME-180-siPGRMC1 cells (Fig. 9B–E). The data suggested that the down-regulation of PGRMC1 could significantly inhibit the proliferation of cervical cancer cells.

3.9. Analysis of cell cycle regulation in siPGRMC1 cells

To further determine the effect of PGRMC1 knockdown on cell cycle regulation of cervical cancer lines, cells were stained with PI and the DNA content was analyzed by flow cytometry. An increased percentage of cells in G1 (78.9%) with concomitant decrease in S (7.9%) and G2/M phases (11.6%) was observed in ME-180-siPGRMC1 cells as compared to ME-180-Mock cells (Fig. 10A). The expression of cell cycle regulatory proteins was also examined by Western blot analysis. The data showed a decreased expression of CDK6 and E2F1 in siPGRMC1 transfected HeLa, CaSki and ME-180 cells as compared to mock cells with simultaneous increase in p21Cip1 expression (Fig. 10B–D). CDK4 expression remained unchanged in siPGRMC1 transfected cell lines. This suggested that PGRMC1 might promote cell proliferation by increasing the expression of G1 phase regulatory proteins with parallel suppression of cyclin-dependent kinase inhibitor expression (Fig. 11).

4. Discussion

Cancer metastasis, a hallmark of malignancy, is the leading cause of mortality in patients with malignant tumors. In case of cervical cancer, prognosis drops dramatically when patients are diagnosed at later stage with lymph node metastasis or local invasion. Therefore, understanding the molecular mechanism of cervical cancer metastasis is critical for developing effective treatment and improving the survival rate.

To investigate the molecular mechanism of cervical cancer metastasis, we established three invasive cervical cancer cell lines HeLa-I5, CaSki-I5 and ME-180-I5 cells which were derived from HeLa, CaSki and ME-180 cells respectively, by selection of cells after transwell invasion assay. Higher rates of migration and proliferation were observed in invasive cells as compared to the respective parental cervical cancer cells. These established invasive cell lines provided a model system to examine cancer metastatic mechanism and to identify potential therapeutic targets.

On the basis of our proteomics data, we demonstrated that PGRMC1 was up-regulated in invasive HeLa-I5 cells compared to HeLa cells. Furthermore, our Western blot data also validated the higher expression of PGRMC1 in invasive CaSki-I5 and ME-180-I5 cells as compared to CaSki and ME-180 cells respectively.

PGRMC1 is a multifunctional, single transmembrane heme-binding protein. It plays a role in several biological processes such as tumor progression, metabolic regulation, and viability control of nerve cells. PGRMC1 is highly expressed in various types of cancers such as lung, breast, ovarian, colon and so on, and facilitates cancer proliferation and promotes chemoresistance. In this study, PGRMC1 was also found to be upregulated in all invasive cervical cancer cell models.

Additionally, to demonstrate the correlation between PGRMC1 expression level and tumor grade, IHC staining of tissue array was performed. Results indicated that higher percentage of PGRMC1 expression was associated with high-grade tumors of all cervical cancer subtypes such as squamous cell carcinoma, cervical adenocarcinoma and metastatic cervical cancer. In general, tumors are graded as 1, 2, 3 or 4 based on the degree of cell differentiation and the rate of cell proliferation. It is an indicator of how quickly a tumor is likely to grow, divide and spread. The low-grade tumors (grade 1 and grade 2) are well-differentiated and have an appearance similar to normal cells indicating a better prognosis, whereas the high-grade tumors (grade 3 and grade 4) are usually poorly- or un-differentiated and look distinctly abnormal. Besides the different degree of differentiation, the high-grade tumors usually grow faster and spread earlier than low-grade tumors implying that the upregulation of PGRMC1 might be correlated with cervical cancer progression and poor prognosis.

We observed that all invasive lines, HeLa-I5, CaSki-I5 and ME-180-I5 exhibited higher migration ability than their respective parental. In order to metastasize, EMT process augments the tumor cell invasiveness, which promotes the cell intravasation by losing cell–cell adhesion and cell motility that leads to the dissemination of tumor cells from its primary site [15]. Moreover, EMT might also contribute towards tumor resistance and cancer cell stemness [16]. In our results, all invasive cervical cancer cells showed decreased expression of epithelial markers with concomitant up-regulation of mesenchymal markers. To further demonstrate the correlation between PGRMC1 and cervical cancer metastasis, siRNA-mediated PGRMC1 knockdowns were performed. After knockdown of PGRMC1, cells showed significant decrease in migration and the expression of EMT markers such as Snail. Snail, a pro-metastatic transcription repressor, is one of the earliest EMT regulators that suppress the expression of epithelial markers. Its expression in tumor is strongly associated with cancer metastasis [17].

Our finding indicates that PGRMC1 might modulate cancer cell migration through EMT regulatory proteins.

Besides showing higher migration ability, HeLa-I5, CaSki-I5 and

ME-180-I5 cell also showed better proliferation than their respective parental cells. Cell cycle analysis revealed a decrease in percentage of cells in G1 phase (49.8%) with parallel increase in S (15.7%) and G2/M (23.5%) phase in HeLa-I5 as compared to HeLa cells. Similarly CaSki-I5 cells also showed a decreased percentage of cells in G1 phase (57.5%) with concomitant increase in S (13.7%) and G2/M (24.0%) phase as compared to CaSki cells. According to our Western blot analysis of cell cycle regulatory proteins, the expressions of CDK6 and E2F1 were up-regulated while p14ARF and p21Cip1 were down-regulated in HeLa-I5 cells as compared to HeLa cells. In CaSki-I5 cells, both p14ARF and p21 Cip1 were down-regulated, while in ME-180-I5 cells only p14ARF was down-regulated with no change in p21Cip1 expression. CDK4 was not differentially expressed among these cell lines. Cyclin-dependent kinases such as CDK4 and CDK6 are essential for the controlling the cell transition from G1 to S phase and their aberrant expression is also a hallmark of cancer, which makes them attractive targets for cancer therapy [18]. A cyclin-dependent kinase inhibitor, p14ARF is an upstream regulator of p53 and act as a tumor suppressor. It induces the premature senescence by activating the p21Cip1 dependent pathway [19]. Some studies suggested that p14ARF is down-regulated in several solid tumors, including breast, urinary bladder, pancreatic and esophageal carcinomas and gliomas [20]. In our study, the down-regulation of p14ARF in invasive cervical cancer cells might promote the cell cycle progress from G1 to S phase. p21Cip1 is also a cyclin-dependent kinase inhibitor and its reduced expression is reported to promote tumor progression in various types of malignant carcinoma [21].

In our case, the decreased expression of p21Cip1 in invasive cervical cancer cells might cause the higher proliferation of the cells. In summary, either up- or down-regulation of G1 phase regulatory proteins and cyclin-dependent kinase inhibitors respectively, might augment the G1 to S and G2/M phase transition of HeLa cells.

siRNA-mediated knockdown of PGRMC1 was performed to gain further insight into its role in cervical cancer progression. Decreased expression of PGRMC1 significantly diminished cell proliferation ability in both parental and invasive cervical cancer cells. In the cell cycle regulation analysis, an increased percentage of cells in G1 phase (78.9%) with a decrease percentage in S (7.9%) and G2/M phase (11.6%) were observed in ME-180-siPGRMC1 cells as compared to ME-180-Mock cells, indicating an arrest of cell cycle in G1 phase [22].

The expression of cycle regulatory proteins corroborated with cell cycle progression data. Knockdown of PGRMC1 was correlated to decreased levels of CDK6 and E2F1 with increased expression of p14ARF and p21Cip1, indicating that PGRMC1 probably modulated cervical cancer progression by regulating the activity of G1 phase regulatory proteins. However, more cell cycle regulatory proteins should be examined to clarify the detail mechanism of cervical cancer progression and metastasis.

In conclusion, our findings provide evidences for an up-regulation of PGRMC1 in both invasive cervical cancer cell lines and high-grade cervical tumors. Furthermore, the data also suggest that PGRMC1 might promote cancer progression and metastasis by modulating the activities of EMT markers and G1 to S phase transition of cell cycle. We propose that PGRMC1 might be a critical diagnostic biomarker and therapeutic target for the treatment of metastatic cervical cancer.

Acknowledgement

This work was supported by the Mackay Memorial Hospital, Taipei, Taiwan with grant number MMH-HB-10711.

Declaration of competing interests

The authors declare no conflicts of interest.

References

[1] P.A. Cohen, A. Jhingran, A. Oaknin, L. Denny, Cervical cancer, Lancet 393 (2019) 169–182.
[2] B.X. Huang, F. Fang, Progress in the study of lymph node metastasis in early-stage cervical cancer, Curr. Med. Sci. 38 (2018) 567–574.
[3] I. Pastushenko, C. Blanpain, EMT transition states during tumor progression and metastasis, Trends Cell Biol. 29 (2019) 212–226.
[4] S. Goossens, N. Vandamme, P. van Vlierberghe, G. Berx, EMT transcription factors in cancer development re-evaluated: Beyond EMT and MET, Biochim Biophys Acta Rev Cancer. 1868 (2017) 584–591.
[5] C.S. Ryu, K. Klein, U.M. Zanger, Membrane Associated Progesterone Receptors: Promiscuous Proteins with Pleiotropic Functions, Focus on Interactions with Cytochromes P450, Front Pharmacol 27 (2017) 159.
[6] H.J. Rohe, I.S. Ahmed, K.E. Twist, R.J. Craven, PGRMC1 (progesterone receptor membrane component 1): a targetable protein with multiple functions in steroid signaling, P450 activation and drug binding, Pharmacol. Ther. 121 (2009) 14–19.
[7] I.S. Ahmed, H.J. Rohe, K.E. Twist, M.N. Mattingly, R.J. Craven, Progesterone receptor membrane component 1 (Pgrmc1): a heme-1 domain protein that promotes tumorigenesis and is inhibited by a small molecule, J. Pharmacol. Exp. Ther. 333 (2010) 564–573.
[8] S.T. Lin, E.W. May, J.F. Chang, R.Y. Hu, L.H. Wang, H.L. Chan, PGRMC1 contributes to doxorubicin-induced chemoresistance in MES-SA uterine sarcoma, Cell. Mol. Life Sci. 72 (2015) 2395–2409.
[9] M.A. Cahill, J.A. Jazayeri, S.M. Catalano, S. Toyokuni, Z. Kovacevic, D.R. Richardson, The emerging role of progesterone receptor membrane component 1 (PGRMC1) in cancer biology, Biochim. Biophys. Acta 1866 (2016) 339–349.
[10] Y. Kabe, T. Nakane, I. Koike, T. Yamamoto, Y. Sugiura, E. Harada, K. Sugase, T. Shimamura, M. Ohmura, K. Muraoka, A. Yamamoto, T. Uchida, S. Iwata, Y. Yamaguchi, E. Krayukhina, M. Noda, H. Handa, K. Ishimori, S. Uchiyama, T. Kobayashi, M. Suematsu, Haem-dependent dimerization of PGRMC1/Sigma-2 receptor facilitates cancer proliferation and chemoresistance, Nat. Commun. 7 (2016) 11030.
[11] M. Willibald, G. Bayer, V. Stahlhut, G. Poschmann, K. Stuhler, B. Gierke, M. Pawlak, H. Seeger, A.O. Mueck, D. Niederacher, T. Fehm, H. Neubauer, Progesterone receptor membrane component 1 is phosphorylated upon progestin treatment in breast cancer cells, Oncotarget. 8 (2017) 72480–72493.
[12] M.A. Cahill, J.A. Jazayeri, Z. Kovacevic, D.R. Richardson, PGRMC1 regulation by phosphorylation: potential new insights in controlling biological activity, Oncotarget. 7 (2016) 50822–50827.
[13] H. Neubauer, S.E. Clare, W. Wozny, G.P. Schwall, S. Poznanovic, W. Stegmann, U. Vogel, K. Sotlar, D. Wallwiener, R. Kurek, T. Fehm, M.A. Cahill, Breast cancer proteomics reveals correlation between estrogen receptor status and differential phosphorylation of PGRMC1, Breast Cancer Res. 10 (2008) R85.
[14] D.F. Schaeffer, D.R. Owen, H.J. Lim, A.K. Buczkowski, S.W. Chung, C.H. Scudamore, D.G. Huntsman, S.S. Ng, D.A. Owen, Insulin-like growth factor 2 mRNA binding protein 3 (IGF2BP3) overexpression in pancreatic ductal adenocarcinoma correlates with poor survival, BMC Cancer 10 (2010) 59.
[15] J.P. Thiery, Epithelial-mesenchymal transitions in tumour progression, Nat. Rev. Cancer 2 (2002) 442–454.
[16] X.X. Jie, X.Y. Zhang, C.J. Xu, Epithelial-to-mesenchymal transition, circulating tumor cells and cancer metastasis: mechanisms and clinical applications, Oncotarget. 8 (2017) 81558–81571.
[17] H.D. Tran, K. Luitel, M. Kim, K. Zhang, G.D. Longmore, D.D. Tran, Transient SNAIL1 expression is necessary for metastatic competence in breast cancer, Cancer Res. 74 (2014) 6330–6340.
[18] M. Zanuy, A. Ramos-Montoya, O. Villacanas, N. Canela, A. Miranda, E. Aguilar, N. Agell, O. Bachs, J. Rubio-Martinez, M.D. Pujol, W.N. Lee, S. Marin, M. Cascante, Cyclin-dependent kinases 4 and 6 control tumor progression and direct glucose oxidation in the pentose cycle, Metabolomics 8 (2012) 454–464.
[19] R. Pare, J.S. Shin, C.S. Lee, Increased expression of senescence markers p14(ARF) and p16(INK4a) in breast cancer is associated with an increased risk of disease recurrence and poor survival outcome, Histopathology 69 (2016) 479–491.
[20] Z. Li, S. Ding, Q. Zhong, G. Li, Y. Zhang, X.C. Huang, Significance of MMP11 and P14(ARF) expressions in clinical outcomes of patients with laryngeal cancer, Int. J. Clin. Exp. Med. 8 (2015) 15581–15590.
[21] J. Adnane, R.J. Jackson, S.V. Nicosia, A.B. Cantor, W.J. Pledger, S.M. Sebti, Loss of p21WAF1/CIP1 accelerates Ras oncogenesis in a transgenic/knockout mammary cancer model, Oncogene 19 (2000) 5338–5347.
[22] G. Xu, H. Wang, W. Li, Z. Xue, Q. Luo, Leukemia inhibitory factor inhibits the proliferation of gastric cancer by inducing G1-phase arrest, J. Cell. Physiol. 234 (2019) 3613–3620.